Heterogeneous Nucleation of Ice on Anthropogenic Organic Particles Collected in Mexico City

D. A. Knopf,[1] B. Wang,[1] A. Laskin,[2] R. C. Moffet,[3] M. K. Gilles[3]

[1]*Institute for Terrestrial and Planetary Atmospheres/School of Marine and Atmospheric Sciences, Stony Brook University, Stony Brook, New York 11794*

[2]*W.R. Wiley Environmental Molecular Sciences Laboratory, Pacific Northwest National Laboratory, Richland, Washington 99352*

[3]*Chemical Sciences Division, Lawrence Berkeley National Laboratory, Berkeley, California 94720*

Manuscript submitted to *Geophysical Research Letters*,

March 22, 2010

Revised April 27, 2010

*Corresponding author, email: *daniel.knopf@stonybrook.edu*

Abstract

This study reports on heterogeneous ice nucleation activity of predominantly organic (or coated with organic material) anthropogenic particles sampled within and around the polluted environment of Mexico City. The onset of heterogeneous ice nucleation was observed as a function of particle temperature (T_p), relative humidity (RH), nucleation mode, and particle chemical composition which is influenced by photochemical atmospheric aging. Particle analyses included computer controlled scanning electron microscopy with energy dispersive analysis of X-rays (CCSEM/EDX) and scanning transmission X-ray microscopy with near edge X-ray absorption fine structure spectroscopy (STXM/NEXAFS). In contrast to most laboratory studies employing proxies of organic aerosol, we show that anthropogenic organic particles collected in Mexico City can potentially induce ice nucleation at experimental conditions relevant to cirrus formation. The results suggest a new precedent for the potential impact of organic particles on ice cloud formation and climate.

Introduction

The ability of aerosols to serve as heterogeneous ice nuclei (IN) for ice crystal formation is one of the least understood microphysical processes which are responsible for large uncertainties in climate modeling [*Baker and Peter*, 2008]. Heterogeneous ice nucleation occurs at warmer temperatures than homogeneous freezing of aqueous inorganic or organic droplets. Thus, IN have a higher propensity to form ice crystals and cirrus clouds. Heterogeneous ice nucleation proceeds by various modes: deposition (ice crystals nucleate from supersaturated water vapor on IN particles), immersion (ice crystals nucleate from supercooled aqueous droplets containing insoluble IN particles), or contact freezing (nucleation of ice crystals induced by collisions of supercooled droplets and IN particles). Cirrus clouds cover ~20% of the Earth's atmosphere and have a predominant warming effect on climate [*Chen et al.*, 2000]. In mixed-phase clouds, IN may govern precipitation, which affects the hydrological cycle. Although the significance of IN is acknowledged, most current climate models do not include processes leading to cloud formation via heterogeneous ice nucleation because they are poorly understood [*Forster et al.*, 2007]. Previously, it was thought that insoluble inorganic particles such as mineral dust were the only relevant IN. Recent studies show that solid $(NH_4)_2SO_4$ particles may act as sufficient IN [*Abbatt et al.*, 2006]. Upper troposphere data suggest that sulfate containing particles are frequently internally mixed with organic constituents [*Murphy et al.*, 1998]. Field measurements in both urban and remote regions indicate that atmospheric aerosols contain a significant fraction of organic material, particularly in the anthropogenically influenced northern hemisphere [*Zhang et al.*, 2007]. However, laboratory studies indicate that organic aerosol proxies are either very efficient (around 115 %RH_{ice}) or, alternatively, very inefficient IN (close to homogeneous freezing). Limited laboratory experiments on the IN ability of crystalline

organic particles [*Kanji et al.*, 2008; *Shilling et al.*, 2006] and soot surrogates [*Mohler et al.*, 2005b] report sufficiently low relative humidity with respect to ice (RH_{ice}) onsets, similar to solid $(NH_4)_2SO_4$ particles. As discussed below, the vast majority of the laboratory studies indicate that carbonaceous particles (soot and organic particles) are inefficient IN under conditions relevant to cirrus formation. Hence, the role of organic material on atmospheric ice nucleation, and thus on cirrus cloud formation, remains elusive.

In this study, we report heterogeneous ice nucleation activity of anthropogenic particles dominated by organics sampled within and around the polluted environment of Mexico City. In comparison to previous studies of urban anthropogenic IN [*Braham and Spyersduran*, 1974; *Szyrmer and Zawadzki*, 1997] we conducted detailed chemical particle analysis paired with ice nucleation experiments over a broad temperature range. We show that these anthropogenic particles can act as IN inducing ice formation at conditions relevant to cirrus formation.

Experimental

Particle Analyses. Particle samples (0.3-2.5 μm in diameter) were collected at T0, T1, and T2 sampling sites during the MILAGRO 2006 campaign [*Molina et al.*, 2007] for subsequent chemical analysis. T0 was inside of the Mexico City metropolitan area; T1 and T2 were northeast from the city, ~35 km and ~60 km, respectively. Particles were collected onto different substrates by a TRAC impactor [*Laskin et al.*, 2006]. Two types of substrates were used: (a) TEM filmed grids for particle analyses using CCSEM/EDX and STXM/NEXAFS, and (b) Si_3N_4 coated silicon wafer chips for ice nucleation experiments. Samples from March 22, 2006, when the northeastern T0→T1→T2 airflow occurred, were

chosen for detailed micro-spectroscopy particle analysis [*Moffet et al.*, 2010] and ice nucleation experiments summarized in Table 1.

Ice nucleation experiments. Ice nucleation onsets were determined using an optical microscope (OM) coupled to an ice nucleation cell (1 mm in diameter, <0.8 cm^3 in volume) allowing control of T_p and RH_{ice} [*Dymarska et al.*, 2006; *Knopf and Lopez*, 2009]. Particles deposited on silicon wafer substrates were exposed to humidified nitrogen (1 SLPM) at a constant dew point (T_d). The cooling rate, 0.1 K min^{-1}, is relevant to rates reported for mid- and low latitude cirrus clouds [*Karcher and Strom*, 2003]. RH_{ice} and RH_{H2O} were derived from the water vapor pressures over water and ice [*Murphy and Koop*, 2005]: $RH_{ice} = p_{H_2O}(T_d) / p_{ice}(T_p)$, $RH_{H_2O} = p_{H_2O}(T_d) / p_{H_2O}(T_p)$. Values of T_p and RH_{ice} corresponding to ice nucleation events were determined at least 3 times for each sample. Subsequent to observed ice nucleation, particle samples were warmed above 273 K to ensure complete sublimation of ice prior to repeating the experiment. Measurement uncertainty was derived from the uncertainty of $\Delta T_d < (\pm 0.15$ K) and of $\Delta T_p < (\pm 0.3$K) resulting in $\Delta RH_{ice} < \pm 10\%$ at 205 K and $\Delta RH_{ice} < \pm 3\%$ at 260 K. The OM technique allows observation of individual ice formation events, visual distinction between ice nucleation modes and water uptake. Water uptake can be detected if the particle size increases by 0.2 μm in diameter due to water adsorption. We report ice formation as deposition nucleation if no water uptake was observed prior to ice crystal formation.

Results and Discussion

In the MILAGRO 2006 campaign, numerous aerosol characterization techniques indicated that secondary organic material was a major component of airborne particles [*Molina et al.*, 2007]. Figure S1 (a) shows a typical SEM image of collected particles. Significant organic

material was associated with every particle measured. This was confirmed by CCSEM/EDX and STXM/NEXAFS micro-spectroscopy analyses of a statistically significant number of particles [*Moffet et al.*, 2010]. Figure S1 (b) shows the particle-type compositions for samples collected at times and locations summarized in Table 1. Close to the source at T0, particles are described as various primary emissions, including dust and sulfate species, coated by secondary organics. As shown in Fig. S1 (b), the particle-type composition at T0 did not change substantially during the day. Transport from T0 to T1 and T2 led to a significant increase in organic material which is attributed to the photochemical formation and processing of secondary organic aerosol [*Doran et al.*, 2007; *Moffet et al.*, 2010; *Molina et al.*, 2007].

Figure 1 (a) summarizes our ice nucleation results along with the previously reported data. The plot includes the ice nucleation onset of a blank substrate indicating the maximum RH_{ice} values achieved in our experiments. To verify the experimental method, the ice nucleation onset was first measured on kaolinite particles. Kaolinite dust is an efficient IN and induces ice formation at RH_{ice} ~115% for T_p in a range of 213-250 K [*Bailey and Hallett*, 2002; *Dymarska et al.*, 2006], conditions which were reproduced in our experiments. Red bars in Fig. 1 (a) show deposition mode onsets of heterogeneous ice nucleation determined for particle samples collected at the T0 site during the time periods indicated in Table 1. Micro-spectroscopy analyses showed that these particles have thick organic coatings resulting from condensational growth of secondary organic material [*Moffet et al.*, 2010]. Particles take up water at T_p > 230 K and ~83% RH_{H2O}, and in some cases, demonstrate immersion mode freezing. Blue bars in Fig. 1 (a) represent heterogeneous ice nucleation onsets determined for particle samples from the T1 and T2 sites located downwind of the urban plume. At these two sites the number of entirely organic particles and extent of organic coating increased

substantially [*Moffet et al.*, 2010]. Similar to T0 particles, deposition ice nucleation was observed at T_p < 230 K. At higher temperatures water uptake and in some cases subsequent immersion freezing occurred. Initial water uptake on T1 and T2 particle samples also occurred at ~83% RH_{H2O}. Overall, ice nucleation onsets observed here are in stark contrast to previous ice nucleation reports applying laboratory proxies of organic particles [e.g. *DeMott et al.*, 1999; *DeMott et al.*, 2009; *Petters et al.*, 2009; *Prenni et al.*, 2001; *Zobrist et al.*, 2006].

As shown in Fig. 1 (a) no significant difference in the measured ice nucleation onsets was observed between particles from different sites or time periods. This supports the premise that the outermost layers of organic material may control the IN propensity of the sampled particles, however, effects of inorganic material cannot be entirely ruled out. In contrast with laboratory studies [*Mohler et al.*, 2008], increasing organic material in the particles did not profoundly affect on the heterogeneous ice nucleation efficiency. This may be attributed to a very thick organic coating, such that deposition of any additional organic material has little impact on heterogeneous ice nucleation. Additional possibilities includes the formation of new IN coupled with the deactivation of IN within the urban plume [*Szyrmer and Zawadzki*, 1997] and particle coagulation. The insensitivity of heterogeneous ice nucleation on additional photochemical processing may facilitate the modeling of ice cloud formation. This is in contrast to the assessment of particle optical properties which can change significantly due to atmospheric aging [*Doran et al.*, 2007].

Figure 1 (b) conveys heterogeneous ice nucleation onset data previously reported using laboratory proxies of organic particles. Most of which display heterogeneous ice nucleation properties substantially different than those reported here. Most literature data fall into two separate classes: very efficient IN which activate at ~115% RH_{ice} or inefficient IN

that activate at RH_{H2O} > 90%. Neither of these indicates heterogeneous ice nucleation activities similar to those measured in particles from Mexico City. Only soot particles coated with multilayers of H_2SO_4 overlap significantly with the heterogeneous ice nucleation onsets reported here. However, laboratory proxies of coated soot particles exhibit a different temperature dependences and nucleation modes (i.e. immersion) compared to the IN activity of particles collected in Mexico City. From our results, we conclude that current laboratory proxies of organic particles are not sufficiently representative to infer heterogeneous ice nucleation activity of anthropogenic organic material. While previous laboratory studies provide insights into the qualitative influence of particle composition on IN properties and validation of nucleation theory, our data strongly suggest that parameterizations based solely on laboratory data for cloud and climate models may not accurately represent atmospheric cloud formation.

In Figure 1 the onset conditions for cirrus formation reported for the Interhemispheric differences in cirrus properties from anthropogenic emissions (INCA) experiment for the northern and southern hemisphere, at mean temperatures of ~225 K, are indicated by sets of black and green dash-dotted horizontal lines, respectively [*Haag et al.*, 2003; *Strom et al.*, 2003]. A clear difference between two hemispheres has been reported in the ice formation onsets. Light grey shaded region indicates continental cirrus formation [*Heymsfield and Miloshevich*, 1995]. Surprisingly, the heterogeneous ice nucleation onsets reported here coincide well with cirrus cloud onset conditions typical for the northern hemisphere, i.e. RH_{ice} > 115% at temperatures of 205-235 K. Analysis of the INCA data concluded that the northern hemisphere cirrus conditions are controlled by homogeneous and selective heterogeneous freezing whereas ice crystals are formed predominantly by homogeneous ice nucleation in the cleaner southern hemisphere [*Haag et al.*, 2003]. Our data suggests that

anthropogenic particles from the urban environment of Mexico City can act as IN under the observed conditions.

Using 2-D projection areas of individual particles, CCSEM/EDX analysis allows an estimation of particle surface area (Table S1). Assuming the surface area of a hemisphere, the upper limit for the heterogeneous ice nucleation rate coefficient of ~200 cm^{-2} s^{-1} is for 205-230 K. Considering particle surface concentrations of ~200 μm^2 cm^{-3} at 2 km altitude above Mexico City [*Lewandowski et al.*, 2010], ice particle production rates are ~$4 \cdot 10^{-4}$ s^{-1} for one cm^3 of air. Hence, under these ambient conditions 24 ice crystals per liter of air can form per minute. This production rate is consistent with typically cirrus ice crystal concentrations [*Lynch et al.*, 2002]. Atmospheric ice crystal numbers can be estimated from the average activated particle fraction, i.e. number of observed IN to total particle number on the substrate, which was approximately 0.002 %. Assuming typical free tropospheric aerosol concentrations of $3 \cdot 10^5$ particles per liter of air, this would produce ~6 ice crystals per liter of air, also consistent with observed cirrus ice crystal concentrations [*Lynch et al.*, 2002].

Further details are provided in the auxiliary materials.

Water uptake at ~83% RH_{H2O} was observed for particles sampled at all locations and times on March 22, 2006 and T_p > 235 K. Laboratory experiments suggest that aerosol particles consisting of multiple miscible organic species and inorganic salts such as $(NH_4)_2SO_4$ possess much lower deliquescence relative humidity (*DRH*) [*Marcolli et al.*, 2004] compared to the corresponding *DRH* values of the individual species. However, *DRH* for organic particle proxies such as malonic acid change by about 30% RH_{H2O} over a temperature range of 50 K [*Braban et al.*, 2003]. This fact and the presence of sulfates on the sampling day could account for higher *DRH* values observed at low temperatures in our

experiments. Uptake of water at these low RH_{H2O} conditions could trigger ice nucleation via immersion freezing.

Summary and Conclusions

We have shown that optical ice nucleation measurements on particle samples collected in field studies and characterized using micro-spectroscopy analyses provide a practical and insightful tool to infer their IN properties. The results presented here indicate that anthropogenic particles dominated by organics can act as sufficient IN under conditions relevant for cirrus cloud formation in contrast to most laboratory studies employing proxies of organic particles. A wide range of field studies indicate that particles containing organics are ubiquitous throughout the troposphere. Our findings are of particular importance given the rapid growth of large cities and increasing urban emissions to the Earth's atmosphere. The results presented in this work call for a re-evaluation of the particle types employed in laboratory experiments on heterogeneous ice nucleation and corresponding parameterizations. Cloud and climate modeling studies may need to consider particles dominated by organic material as potential IN involved in cirrus cloud formation.

Acknowledgements

The SBU research group acknowledges support by the NOAA Climate Program Office, Atmospheric Composition & Climate Program, Grant NA08OAR4310545. The PNNL and LBNL groups acknowledge support from the Atmospheric System Research of the Department of Energy's office of Biological and Environmental Research. R. C. Moffet acknowledges partial support from a Lawrence Berkeley National Laboratory Glenn T. Seaborg Fellowship. The Advanced Light Source is supported by the Director, Office of

Science, Office of Basic Energy Sciences, of the U.S. Department of Energy. The Environmental Molecular Sciences Laboratory, a national scientific user facility sponsored by the Department of Energy's Office of Biological and Environmental Research at Pacific Northwest National Laboratory. PNNL is operated by the U.S. Department of Energy by Battelle Memorial Institute. The authors gratefully acknowledge help of Y. Desyaterik and R.J. Hopkins at the sampling sites.

Work done using the Advanced Light Source was supported by the U.S. Department of Energy under Contract No. DE-AC03-05CH11231.

Table 1 Location and Times of Particle Samples Used for Nucleation Studies.

(MILAGRO 2006 field campaign)

Sample Location	Local Time of Sampling	CCSEM/EDX, STXM/NEXAFS Particle Analyses	Ice Nucleation Experiments
T0	05:20 - 05:35		X
T0	05:35 - 05:50	X	
T0	10:35 - 10:50	X	
T0	12:20 - 12:35		X
T0	12:35 - 12:50	X	
T0	14:20 - 14:35		X
T1	08:35 - 08:50	X	
T1	13:00 - 13:15	X	
T1	13:45 - 14:00		X
T1	18:00 - 18:15	X	
T2	14:15 - 14:30		X
T2	14:30 - 14:45	X	
T2	19:30 - 19:45	X	

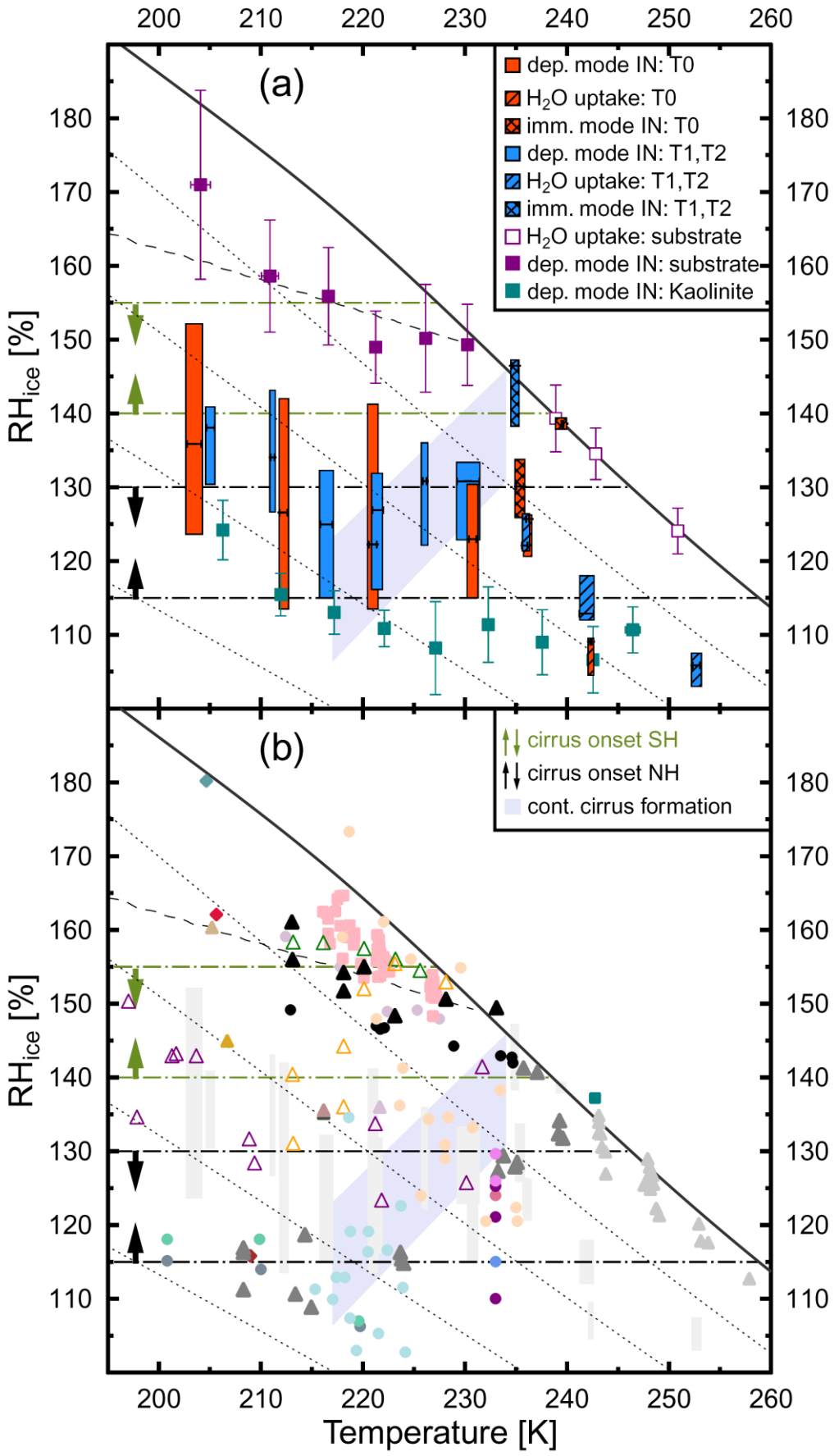
(a)
(b)
dep. mode IN: T0
H2O uptake: T0
imm. mode IN: T0
dep. mode IN: T1,T2
H2O uptake: T1,T2
imm. mode IN: T1,T2
H2O uptake: substrate
dep. mode IN: substrate
dep. mode IN: Kaolinite
cirrus onset SH
cirrus onset NH
cont. cirrus formation
RHice [%]
Temperature [K]
200
210
220
230
240
250
260
110
120
130
140
150
160
170
180

Figure 1. Panel (a). Experimentally determined range of heterogeneous ice nucleation onsets of particles sampled in (■) and around (■) Mexico City (Table 1) indicated by colored bars. Corresponding shaded (▨, ▨), and hatched (▩, ▩) bars represent conditions at which water uptake and immersion mode freezing were observed, respectively. The horizontal solid lines within the bars indicate the median IN onset calculated from multiple observations. Water uptake (□) and ice formation (■) on blank substrates indicate no substrate effect on the ice nucleation experiments. Heterogeneous ice nucleation onsets for kaolinite particles are shown (■). The solid black line indicates water saturation (100% RH_{H2O}) and diagonal dotted lines indicate levels of 90, 80, 70, and 60% RH_{H2O} from the top to the bottom left, respectively. The dashed line indicates the theoretical [*Koop et al.*, 2000] homogeneous freezing limit corresponding to a homogeneous ice nucleation rate coefficient of about $5 \cdot 10^9$ cm^{-3} s^{-1}. Light grey shaded area indicates bounds of continental cirrus formation [*Heymsfield and Miloshevich*, 1995]. The RH_{ice} ranges within the horizontal dash-dotted lines (emphasized by corresponding arrows) indicate the lower limits for cirrus formation conditions in northern (black) and southern hemisphere (green) [*Strom et al.*, 2003]. Panel (b). Reported heterogeneous ice nucleation onsets for laboratory generated proxies of organic particles are shown using the following symbols: ▲- soot aged by O_3 [*Dymarska et al.*, 2006]; ●, ● - maleic acid and mixed maleic acid-ammonium sulfate particles[1] [*Shilling et al.*, 2006]; ●, ● - glutaric acid and mixed glutaric acid-ammonium sulfate particles particles[1] [*Baustian et al.*, 2010]; ●, ●, ●, ● - leonardite, oxalic acid, sodium humic acid, and octyl-silica[1] [*Kanji et al.*, 2008]; △, ▲ - soot coated with sulfuric acid, and uncoated soot particles [*Mohler et al.*, 2005b]; ▲, ▲ - soot containing different amounts of sulfur [*Mohler et al.*, 2005a]; ◆, ◆, ◆ - Arizona test dust coated by secondary organic aerosol (SOA), illite coated by SOA, pure SOA [*Mohler et al.*, 2008]; ● - crystalline oxalic acid in aqueous solution[1] [*Zobrist et al.*, 2006]; ● - adipic acid [*Prenni et al.*, 2001]; ▲, △, △ – soot, soot coated with a monolayer, and multiple layers of sulfuric acid [*DeMott et al.*, 1999]; ▲, ▲, ▲ - three different types of oxidized soot surrogates [*Koehler et al.*, 2009]; ■, ■ -

biomass burning particles from two different studies [*DeMott et al.*, 2009; *Petters et al.*, 2009]. [1]These studies employed particles up to 10 μm in diameter. Ice nucleation data of this study are indicated as light grey bars for comparison. All other lines are the same as in panel (a).

References:

Abbatt, J. P. D., S. Benz, D. J. Cziczo, Z. Kanji, U. Lohmann, and O. Mohler (2006), Solid ammonium sulfate aerosols as ice nuclei: A pathway for cirrus cloud formation, *Science*, *313*(5794), 1770-1773, doi: 10.1126/science.1129726.

Bailey, M., and J. Hallett (2002), Nucleation effects on the habit of vapour grown ice crystals from-18 to-42 degrees C, *Q. J. R. Meteor. Soc.*, *128*(583), 1461-1483, doi: 10.1002/qj.200212858304.

Baker, M. B., and T. Peter (2008), Small-scale cloud processes and climate, *Nature*, *451*(7176), 299-300, doi: 10.1038/nature06594.

Baustian, K. J., M. E. Wise, and M. A. Tolbert (2010), Depositional ice nucleation on solid ammonium sulfate and glutaric acid particles, *Atmos. Chem. Phys.*, *10*(5), 2307-2317.

Braban, C. F., M. F. Carroll, S. A. Styler, and J. P. D. Abbatt (2003), Phase transitions of malonic and oxalic acid aerosols, *J. Phys. Chem. A*, *107*, 6594-6602, doi: 10.1021/jp034483f.

Braham, R. R., and P. Spyersduran (1974), Ice Nucleus Measurements in an urban Atmosphere, *J. Appl. Meteorol.*, *13*(8), 940-945.

Chen, T., W. B. Rossow, and Y. C. Zhang (2000), Radiative effects of cloud-type variations, *J. Climate*, *13*(1), 264-286.

DeMott, P. J., Y. Chen, S. M. Kreidenweis, D. C. Rogers, and D. E. Sherman (1999), Ice formation by black carbon particles, *Geophys. Res. Lett.*, *26*(16), 2429-2432.

DeMott, P. J., M. D. Petters, A. J. Prenni, C. M. Carrico, S. M. Kreidenweis, J. L. Collett, and H. Moosmuller (2009), Ice nucleation behavior of biomass combustion particles at cirrus temperatures, *J. Geophys. Res.*, *114*, D16205, doi: 10.1029/2009jd012036.

Doran, J. C., et al. (2007), The T1-T2 study: evolution of aerosol properties downwind of Mexico City, *Atmospheric Chemistry and Physics*, *7*(6), 1585-1598.

Dymarska, M., B. J. Murray, L. Sun, M. Eastwood, D. A. Knopf, and A. K. Bertram (2006), Deposition ice nucleation on soot at temperatures relevant for the lower troposphere, *J. Geophys. Res.*, *111*, D04204, doi: 10.1029/2005jd006627.

Forster, P., et al. (2007), in *Climate Change 2007: The Physical Science Basis. Contribution of Working Group I to the Fourth Assessment Report of the Intergovernmental Panel on Climate Change*, edited by S. Solomon, D. Qin, M. Manning, Z. Chen, M. Marquis, K. B. Averyt, M. Tignor and H. L. Miller, pp. 131-234, Cambridge University Press.

Haag, W., B. Karcher, J. Strom, A. Minikin, U. Lohmann, J. Ovarlez, and A. Stohl (2003), Freezing thresholds and cirrus cloud formation mechanisms inferred from in situ measurements of relative humidity, *Atmos. Chem. Phys.*, *3*, 1791-1806.

Heymsfield, A. J., and L. M. Miloshevich (1995), Relative humidity and temperature influences on cirrus formation and evolution: Observations from wave clouds and FIRE II, *J. Atmos. Sci.*, *52*(23), 4302-4326.

Kanji, Z. A., O. Florea, and J. P. D. Abbatt (2008), Ice formation via deposition nucleation on mineral dust and organics: dependence of onset relative humidity on total particulate surface area, *Env. Res. Lett.*, *3*(2), Artn 025004, doi: 10.1088/1748-9326/3/2/025004.

Karcher, B., and J. Strom (2003), The roles of dynamical variability and aerosols in cirrus cloud formation, *Atmos. Chem. Phys.*, *3*, 823-838.

Knopf, D. A., and M. D. Lopez (2009), Homogeneous ice freezing temperatures and ice nucleation rates of aqueous ammonium sulfate and aqueous levoglucosan particles for relevant atmospheric conditions, *Phys. Chem. Chem. Phys.*, *11*(36), 8056-8068, doi: 10.1039/B903750k.

Koehler, K. A., P. J. DeMott, S. M. Kreidenweis, O. B. Popovicheva, M. D. Petters, C. M. Carrico, E. D. Kireeva, T. D. Khokhlova, and N. K. Shonija (2009), Cloud condensation

nuclei and ice nucleation activity of hydrophobic and hydrophilic soot particles, *Phys. Chem. Chem. Phys.*, *11*(36), 7906-7920, doi: 10.1039/b905334b.

Koop, T., B. P. Luo, A. Tsias, and T. Peter (2000), Water activity as the determinant for homogeneous ice nucleation in aqueous solutions, *Nature*, *406*(6796), 611-614, doi: 10.1038/35020537

Laskin, A., J. P. Cowin, and M. J. Iedema (2006), Off-line analysis of individual environmental particles using modern methods of electron microscopy and X-ray microanalysis, *Journal of Electron Spectroscopy and Related Phenomena*, *150*, 260-274.

Lewandowski, P. A., W. E. Eichinger, H. Holder, J. Prueger, J. Wang, and L. I. Kleinman (2010), Vertical distribution of aerosols in the vicinity of Mexico City during MILAGRO-2006 Campaign, *Atmos Chem Phys*, *10*(3), 1017-1030.

Lynch, D. K., K. Sassen, D. C. Starr, and G. Stephens (2002), *Cirrus*, Oxford University Press, New York.

Marcolli, C., B. P. Luo, and T. Peter (2004), Mixing of the organic aerosol fractions: Liquids as the thermodynamically stable phases, *J. Phys. Chem. A*, *108*(12), 2216-2224, doi: 10.1021/jp036080l.

Moffet, R. C., et al. (2010), Microscopic characterization of carbonaceous aerosol particle aging in the outflow from Mexico City *Atmos. Chem. Phys.*, *10*, 961–976.

Mohler, O., C. Linke, H. Saathoff, M. Schnaiter, R. Wagner, A. Mangold, M. Kramer, and U. Schurath (2005a), Ice nucleation on flame soot aerosol of different organic carbon content, *Meteorol. Z.*, *14*(4), 477-484, doi: Doi 10.1127/0941-2948/2005/0055.

Mohler, O., S. Benz, H. Saathoff, M. Schnaiter, R. Wagner, J. Schneider, S. Walter, V. Ebert, and S. Wagner (2008), The effect of organic coating on the heterogeneous ice nucleation

efficiency of mineral dust aerosols, *Env. Res. Lett.*, *3*(2), Artn 025007, doi: Doi 10.1088/1748-9326/3/2/025007.

Mohler, O., et al. (2005b), Effect of sulfuric acid coating on heterogeneous ice nucleation by soot aerosol particles, *J. Geophys. Res.*, *110*, D11210, doi: 10.1029/2004JD005169.

Molina, L. T., S. Madronich, J. S. Gaffney, H. B. Singh, U. Pöschl, and (2007), ACP Special Issue: MILAGRO/INTEX-B 2006, *Atmos. Chem. Phys.*

Murphy, D. M., and T. Koop (2005), Review of the vapour pressures of ice and supercooled water for atmospheric applications, *Q. J. R. Meteor. Soc.*, *131*(608), 1539-1565, doi: 10.1256/Qj.04.94.

Murphy, D. M., D. S. Thomson, and T. M. J. Mahoney (1998), In situ measurements of organics, meteoritic material, mercury, and other elements in aerosols at 5 to 19 kilometers, *Science*, *282*(5394), 1664-1669.

Petters, M. D., et al. (2009), Ice nuclei emissions from biomass burning, *J. Geophys. Res.*, *114*, D07209, doi: 10.1029/2008jd011532.

Prenni, A. J., P. J. DeMott, S. M. Kreidenweis, D. E. Sherman, L. M. Russell, and Y. Ming (2001), The effects of low molecular weight dicarboxylic acids on cloud formation, *J. Phys. Chem. A*, *105*(50), 11240-11248, doi: 10.1021/jp012427d.

Shilling, J. E., T. J. Fortin, and M. A. Tolbert (2006), Depositional ice nucleation on crystalline organic and inorganic solids, *J. Geophys. Res.*, *111*(D12), D12204, doi: 0.1029/2005jd006664.

Strom, J., et al. (2003), Cirrus cloud occurrence as function of ambient relative humidity: a comparison of observations obtained during the INCA experiment, *Atmos. Chem. Phys.*, *3*, 1807-1816.

Szyrmer, W., and I. Zawadzki (1997), Biogenic and anthropogenic sources of ice-forming nuclei: A review, *Bull. Amer. Meteorol. Soc., 78*(2), 209-228.

Zhang, Q., et al. (2007), Ubiquity and dominance of oxygenated species in organic aerosols in anthropogenically-influenced Northern Hemisphere midlatitudes, *Geophys. Res. Lett.*, *34*(13), Artn L13801, doi: 10.1029/2007gl029979.

Zobrist, B., et al. (2006), Oxalic acid as a heterogeneous ice nucleus in the upper troposphere and its indirect aerosol effect, *Atmos. Chem. and Phys.*, *6*, 3115-3129.

Derivation of heterogeneous ice nucleation rate coefficient.

The total particle surface area accessible in our ice nucleation experiments is determined under the assumption that particles are hemispheres. This assumption may lead to an underestimation of the particle surface area and thus results in an upper limit of the heterogeneous ice nucleation rate coefficient, J_{het}. J_{het} given in units cm^{-2} s^{-1} was derived from the exposed particle surface area and the time period the particles were exposed to RH_{ice} > 100% until the first freezing event was observed. This calculation yields J_{het} values of about 3-371cm^{-2} s^{-1} for lowest to highest observed RH_{ice} onset values, respectively, for the temperature range of 205-230 K. This procedure follows the methods employed by previous studies [e.g. *Dymarska et al.*, 2006; *Eastwood et al.*, 2008]. Ice particle production rates, P_{ice}, can be derived from $P_{ice}=J_{het}\cdot A_{aerosol}$, where $A_{aerosol}$ is the aerosol surface area per cm^3 of air.

Derivation of activated particle fraction.

CCSEM/EDX analysis allows for an estimation of the particle number concentration on the substrate. The activated particle fraction is the number of observed ice crystals to total particle number for a particular particle temperature. This calculation yields activated particle fractions of about 0.0008-0.01% for lowest to highest observed RH_{ice} onset values, respectively, for the temperature range of 205-230 K. Ice particle concentrations can be derived by multiplying the activated particle fraction by typical tropospheric aerosol background number concentrations. It is important to note that this approach does not yield a rate, i.e. the time dependence of the nucleation process is not taken into account.

References

Dymarska, M., B. J. Murray, L. Sun, M. Eastwood, D. A. Knopf, and A. K. Bertram (2006), Deposition ice nucleation on soot at temperatures relevant for the lower troposphere, *J.Geophys. Res.*, *111*, D04204, doi: 10.1029/2005jd006627.

Eastwood, M. L., S. Cremel, C. Gehrke, E. Girard, and A. K. Bertram (2008), Ice nucleation on mineral dust particles: Onset conditions, nucleation rates and contact angles, *J. Geophys. Res.*, *113*, D22203, doi: 10.1029/2008jd010639.

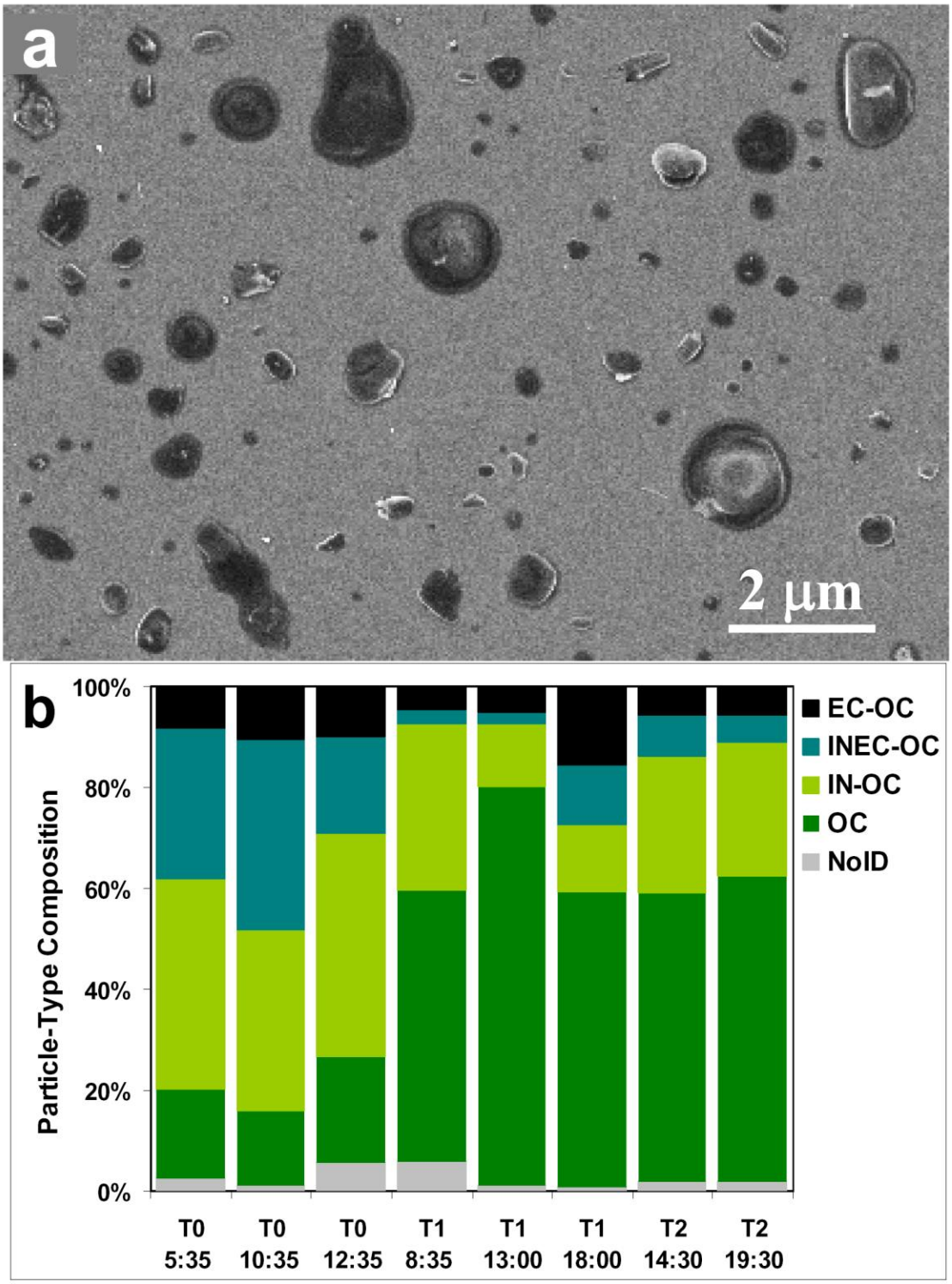

Figure S1 Summary of the microscopy and micro-spectroscopy analyses of particles collected in the MILAGRO 2006 study. Panel (a) shows particle morphology revealed by SEM. The dark areas indicate organic material. The image illustrates particles collected at T2 - 19:30. Panel (b)

shows results of the particle-type classification for 8 analyzed samples from March 22, 2006 collected at T0, T1, and T2 sampling sites. Particle types are defined based on the results of STXM/NEXAFS micro-spectroscopy analysis that distinguishes the following components within individual particles: OC – organic carbon, IN – inorganic material, EC – elemental carbon [*Moffet et al.*, 2010]. Combinations of these components are used to define four major particle classes. Notably, the OC component is present in all particles. NoID class corresponds to particles that could not be assigned to a specific class because of their low signal to noise.

Table SI. Particle substrate number density and total surface area estimates based on CCSEM analysis†.

1. Sample Location and Time.	2. Sample area observed in IN experiment, S_{IN}, mm^2	3. Sample area inspected by CCSEM analysis, S_{CCSEM}, mm^2	4. Number of particles found by CCSEM, N_{CCSEM},	5. Particle total 2D projection area, A_{2D}, mm^2	6. Particles on substrate density, d_{CCSEM}, mm^{-2}	7. Fraction of substrate area covered by particles, F	8. Mean particle diameter, D_p, µm	9. Total particle surface area for IN experiment, SA_{part}, mm^{-2}
T0, 05:20-05:35	0.675							
T0, 05:35-05:50		$1.62 \cdot 10^{-2}$	6100	$9.40 \cdot 10^{-4}$	$3.77 \cdot 10^{5}$	$5.80 \cdot 10^{-2}$	0.443	$8.00 \cdot 10^{-2}$
T0, 12:20-12:35	0.625							
T0, 12:35-12:50		$1.62 \cdot 10^{-2}$	2500	$6.20 \cdot 10^{-4}$	$1.54 \cdot 10^{5}$	$3.83 \cdot 10^{-2}$	0.562	$4.77 \cdot 10^{-2}$
T0, 14:20-14:35	0.649							
T0, 14:35-14:50		$4.32 \cdot 10^{-3}$	600	$2.00 \cdot 10^{-4}$	$1.39 \cdot 10^{5}$	$4.63 \cdot 10^{-2}$	0.651	$6.25 \cdot 10^{-2}$
T1, 13:00-13:15								
T1, 13:45-14:00	0.690	$2.16 \cdot 10^{-2}$	6750	$1.40 \cdot 10^{-3}$	$3.13 \cdot 10^{5}$	$6.48 \cdot 10^{-2}$	0.514	$8.10 \cdot 10^{-2}$
T2, 14:15-14:30	0.624							
T2, 14:30-14:35		$5.40 \cdot 10^{-3}$	800	$2.75 \cdot 10^{-4}$	$1.48 \cdot 10^{5}$	$5.09 \cdot 10^{-2}$	0.662	$6.61 \cdot 10^{-2}$

1. Location (T0, T1, T2 sampling sites) and local time of sampling.
2. $\mathbf{S_{IN}}$ – total area of the sample observed during IN experiment. The area was calculated using the optical microscopy image.

3-5. During the CCSEM analysis a matrix of fields-of-view is set over the sample with deposited particles. The sample is then automatically inspected on a field-by-field basis. In each field-of-view, particles are recognized by an increase of the mixed BSE/TED signal above a pre-selected threshold level (see *Laskin et al,* 2006 for details). $\boldsymbol{S_{CCSEM}}$ - total area of the sample inspected by CCSEM analysis. The area is determined as a total area over carbon film with particles observed in all CCSEM inspected fields-of-view. N_{CCSEM} - total number of particles reported by the CCSEM analysis. A_{2D} – total 2D projection area of all particles reported by the CCSEM analysis.

6. d_{CCSEM} - lateral density of particles over the sample area is estimated as: $d_{CCSEM} = N_{CCSEM}/S_{CCSEM}$
7. F - fraction of substrate area covered by particles is estimated as: $F = A_{2D}/S_{CCSEM}$
8. D_p - estimated mean particle diameter, assuming circles as particle projection areas: $D_p = \sqrt{\frac{4A_{2D}}{\pi N_{CCSEM}}}$
9. SA_{part} – total particle surface area monitored in IN experiment, assuming particles are hemispheres with diameter D_p: $SA_{part} = \frac{\pi D_p^2}{2} S_{IN} N_{CCSEM}$

† CCSEM/EDX analysis of particles was performed over the samples collected on Copper 400 mesh TEM grids coated with Carbon type B film (Ted Pella, Inc.).